Energy 170 (2019) 592–603

Contents lists available at ScienceDirect

Energy

journal homepage: www.elsevier.com/locate/energy

Development of net energy ratios and life cycle greenhouse gas emissions of large-scale mechanical energy storage systems

S. Kapila, A.O. Oni, E.D. Gemechu, A. Kumar*

Department of Mechanical Engineering, University of Alberta, 10-263 Donadeo Innovation Centre for Engineering, Edmonton, Alberta T6G 1H9, Canada

A R T I C L E I N F O

Article history:
Received 20 March 2018
Received in revised form
28 November 2018
Accepted 24 December 2018
Available online 26 December 2018

Keywords:
Compressed air energy storage
Greenhouse gas emissions
Large energy storage systems
Life cycle assessment
Net energy ratio
Pumped hydroelectric storage

A B S T R A C T

In this study, a process model was developed to determine the net energy ratios and life cycle greenhouse gas emissions of three energy storage systems: adiabatic and conventional compressed air energy storage and pumped hydroelectric energy storage, with estimated capacities of 118, 81, and 60 MW, respectively. The net energy ratios were calculated as ratios of net energy outputs to the total net energy inputs. The greenhouse gas emissions associated with construction, operation, decommissioning life cycle stages of the energy storage systems were evaluated. The net energy ratios for the adiabatic and conventional compressed air energy storage and pumped hydroelectric energy storage are 0.702, 0.542, and 0.778, respectively. The respective life cycle greenhouse gas emissions in g CO_2 eq./kWh are 231.2, 368.2, and 211.1. The emissions are highly dominated by the operational stage in all the energy storage systems. It was also observed that energy consumption in the form of electricity is the key driver, while the contributions due to the use of material are minimal. Sensitivity and uncertainty analysis was also performed. The results help in understanding the comparative net energy ratios and emission footprints of various energy storage systems in order to make an informed decision.

1. Introduction

Greenhouse gas (GHG) emissions from industrial activities are one of the main contributors to global warming. In 2010, electricity and heat production accounted for 25% of the global GHG emissions [1,2]. Most of the emissions come from the use of fossil fuels, as coal and natural gas still dominate in the power sector [3]. Thus, there is rapidly growing interest in renewable energy production technologies as they have high potential to mitigate climate change. To achieve the International Energy Agency's (IEA) two-degree scenario target, renewable energy production will need to meet 74% of global electricity demand by 2060 [4]. Large-scale mechanical energy storage systems (MESSes) such as pumped hydroelectric and conventional and adiabatic compressed air energy storage systems have the potential to play a vital role in achieving the target.

A MESS stores excess electricity from the grid when there is less demand and releases electricity when demand exceeds supply [5,6]. A MESSes is an intermediate system that integrates renewable sources into existing electricity grids and thus helps lower overall GHG emissions. That said, the life cycle stages (construction, operation, and decommissioning) of a MESS require material and energy inputs, and there are associated GHG emissions. Therefore, to evaluate the environmental impacts and benefits associated with different MESSes, it is imperative to perform a life cycle assessment (LCA) of these systems. Besides the life cycle GHG emissions, the net energy ratio, which can be used to determine the energy performance of the different MESSes, is also an important factor to consider. The net energy ratio is used to measure the effectiveness of a technology in terms of providing energy to an economy. It is used to evaluate the difference between total energy input to available output, thus accounting for the impact of energy consumption. A technology with a larger net energy ratio is mostly preferred. Any technology with a low or negative net energy ratio cannot compete in the open marketplace with other energy alternatives with higher net energy ratios. In this study, both life cycle GHG emissions and net energy ratio are considered as metrics for assessing the environmental impact and energy sustainability of the MESSes studied, respectively.

A few studies are available on LCA and NER of MESSes. These studies have demonstrated the knowledge of LCA and/or NER to various energy storage systems. In earlier work by Denholm and Kulcinski [7], life cycle energy requirements, GHG emissions, and

* Corresponding author.
E-mail address: Amit.Kumar@ualberta.ca (A. Kumar).

https://doi.org/10.1016/j.energy.2018.12.183

Acronyms

A-CAES	Adiabatic compressed air energy storage
C-CAES	Conventional compressed air energy storage
CAES	Compressed air energy storage
CLP	Climate Leadership Plan
DEF	Direct emission factor
ESS	Energy storage system
GHG	Greenhouse gas
IEA	International Energy Agency
kW	Kilowatt
kWh	Kilowatt hour
LCA	Life cycle assessment
NER	Net energy ratio
NG	Natural gas
MW	Megawatt
MWh	Megawatt-hour
PHS	Pumped hydroelectric storage
TEF	Total emission factor

NERs of pumped hydroelectric storage (PHS), compressed air energy storage (CAES), and battery energy storage (BES) systems were examined using a hybrid LCA approach, a combination of process chain analysis and economic input/output LCA. Process chain analysis was applied for processes where material and energy data are available, while a highly aggregated EIO approach was used for processes in which complete inventory data were not available. This work was primarily carried out to compare energy input and associated GHG emissions of PHS with CAES and BES when coupled with fossil, renewable, and nuclear energy sources. Oliveira et al. [12] carried out a comparative environmental impact of a range of storage technologies using exiting life cycle inventory data from various project sources. In some cases technical data at the project stage was extrapolated to process-based inventory using the Ecoinvent database. The study applied the ReCiPe impact assessment method to translate the inventory values to a number of environmental impact indicators. The NER as energy performance was not explicitly evaluated. Akhil et al. [15] comprehensively reviewed and compared life cycle GHG emissions from different hydro facilities including pumped hydroelectric plants. Bouman et al. [16] conducted LCA of a CAES plant integrated with offshore wind plants through a cradle-to-grave approach. The results show that integrating conventional compressed air energy storage (C-CAES) with a wind plant significantly increases the environmental impacts whereas adiabatic compressed air energy storage (A-CAES) only moderately increases these impacts. Other studies such as those by Hiremath et al. [8] and Rydh et al. [9] conducted comparative assessments of battery energy storage systems for stationary applications and showed that using batteries as storage mediums has significant impacts on overall GHG emissions. The work by Jing et al. [10] focused on thermal energy storage systems for combined cooling, heating, and power system applications. The system operated following the thermal load operational strategy wherein excess electricity produced is stored for future use and this strategy has a lower pollutant impact and more energy-saving potential. Eduard et al. [11] performed a comparative assessment of thermal energy storage systems for solar power plants. A system using solid media (i.e., concrete) has fewer environmental impacts than a system using liquid media (i.e., molten salt). A few other studies considered a bundle of storage technologies together [12–14]. The results indicate that compared to other storage systems batteries have higher impacts during their construction and end-of-life phases and lower impacts during operation. Welsh et al. [17] conducted the environmental and economic assessment of borehole thermal energy storage in district heating systems. A medium deep borehole thermal energy system combined with a large solar thermal collector field and a small combined heat and power (CHP) can be a cheap substitute to large CHPs for mitigating GHG emissions in district heating systems. Tschiggerl et al. [18] conducted an LCA to compare the environmental impacts of different power-to-gas business scenarios. The source of energy is a vital parameter in determining the environmental performance of a power-to-gas plant. Guney and Tepe [19] presented a broad view on assessment and comparison of energy storage systems. An earlier study by those authors focused on the techno-economic assessment of ESS but did not look at the environmental impacts [19].

Although most of the above studies consolidate the increasing interest in renewables and storage technologies, some do not provide detailed information on the method used and how the results are obtained. The majority of the studies are based on high level aggregated data, which does not accurately measure or estimate the input and output requirement of a specific product. In this study, engineering first principles were implemented to design the storage systems and estimate energy and material use. Again, some studies did not consider a holistic LCA of the system studied; they usually omitted the decommissioning and/or construction phase. A holistic evaluation of the life cycle GHG emissions and NER is required to understand the overall environmental performance of the storage systems. In addition, results based on point estimates or hotspot analysis may not provide such comprehensive information due to the level of uncertainty that may exist in some of the underlying process variables. Analyses of sensitivity and uncertainty are important for the evaluation of these models because the interrelationship among underlying process parameters and their corresponding variability can be revealed. This can help in understanding the impact of energy consumption and GHG emissions, thus providing useful information for decision makers. Furthermore, no detailed comparative study of large MESSes (PHS, C-CAES, and A-CAES) has been reported in previous literature; such a study can provide both qualitative and quantitative analyses for decision making. This study aims to fill these gaps.

The overall aim of this study is to use a comprehensive, bottom-up approach to compile a life cycle inventory and estimate the GHG emissions and the NERs for selected MESSes considering their specific system sizes in order to provide information to policymakers and governments to help them make informed decisions. The specific objectives are to:

- Develop the NERs for three large mechanical storage systems (A-CAES, C-CAES, and PHS), the leading candidates for large-scale storage applications such as load shifting and spinning reserves for the integration of large capacities of renewable technologies with the utility grid;
- Estimate the life cycle GHG emissions and NER of these energy storage systems;
- Perform sensitivity and uncertainty analyses to provide ranges of estimates for life cycle GHG emissions and NERs;
- Conduct a case study for various provinces in Canada with respect to the integration of the storage systems and associated GHG emissions.

2. Method

Fig. 1 shows the five-stage methodological framework of the study. The goal and scope definition stage address the following points: the reasons for conducting LCA, detailed description of the storage systems considered in the assessment, the LCA methodology, the system boundary considered, and the functional unit used as a base on comparison. In the design stage, first engineering principles were applied to design each storage system. A process simulation model for each storage system is carefully developed to ensure the interactions between components/unit operations, and their performances represent real life processes. Each piece of equipment is then sized to determine material and energy requirements. The life cycle inventory stage comprises the material and energy requirements at each life cycle stage of the storage systems. The fourth stage translates input and output requirements into GHG emissions as eq-CO_2 per the defined functional unit. The NER as a ratio of total energy produced to total energy consumed is also determined at this stage. The last stage deals with sensitivity and uncertainty analyses for better interpretation of the GHG emissions and NER results. The following sections discuss thoroughly the main components of each stage of the framework.

2.1. Goal and scope definition

The aim of the study is to evaluate the life cycle GHG emissions and NER of large-scale storage systems and to conduct a comparative LCA of three energy storage systems, A-CAES, C-CAES, and PHS. Each storage technology is described in detail below [20].

2.1.1. Pumped hydroelectric storage (PHS)

PHS can be an open loop or a closed loop system. When either or both reservoirs are connected to a free-flowing water source, it is an open loop system. When both reservoirs are isolated from a free-flowing water source, it is a closed loop system. The flow diagram of a closed loop PHS is presented in Fig. 2. The main components of a PHS facility are: the pump turbine (used to pump the water from lower reservoir to upper reservoir and vice versa), the motor/generator (the point where energy moves in and out of the system), the reservoirs (used to store the water), and the valves to regulate the water flow.

When the electricity demand is less than the supply, the excess electricity from the grid is used to pump the water from the lower reservoir to the upper reservoir. When the electricity demand is more than the supply, the PHS uses the gravitational potential energy of water in the upper reservoir to operate the turbine, generating electricity and adding it back to the grid.

The power output (P) of the pump turbine is proportional to the water head available (h) and the flow rate (Q) of water.

$$P = \eta * \rho * g * Q * h \tag{1}$$

where η, is the overall efficiency of the pump turbine and ρ is the density of water.

2.1.2. Conventional compressed air energy storage (C-CAES)

The flow diagram of a C-CAES plant is presented in Fig. 3. The main components of a C-CAES plant are the compressors (to compress the air), intercoolers to remove heat content of the compressed air, a storage medium (to store the compressed air), combustors (to supply compressed air with energy content by burning natural gas), and the turbine (to generate electricity).

C-CAES is a hybrid storage system that works similar to conventional gas turbine technology. It requires the combustion of natural gas in its operational phase to produce electricity. When electricity demand is less than supply, the excess electricity from the grid is used to compress air for storage in an underground cavern and later used to combust natural gas and supply electricity when there is a shortage. The compressed air is preheated with exhaust gases in the recuperator before entering the combustor.

The temperatures throughout the system were determined using principles of energy balance through ideal gas polytropic relation [20]. The power delivered by the turbine ($P_{turbine}$) was calculated from mass flow rate of air $\dot{m}_{air}$ and temperature differential across turbine:

$$P_{turbine} = C_{p,air} * \dot{m}_{air} * (T_{in,\,turbine} - T_{out,turbine}) \tag{2}$$

where $C_{p,air}$ is the specific heat of air.

2.1.3. Adiabatic compressed air energy storage (A-CEAS)

The flow diagram of A-CAES is presented in Fig. 4. The main components of an A-CEAS system are the compressors (to compress the air), heat exchangers (which remove the heat content of the compressed air and supply it back during electricity generation), a storage medium (to store the compressed air), heat transfer fluid (to facilitate the removal of energy content from the compressed air and supply), and turbines (to generate electricity).

An A-CAES system does not combust natural gas for its operation; instead it uses a thermal energy storage system to store the heat generated when the air is compressed. The thermal energy

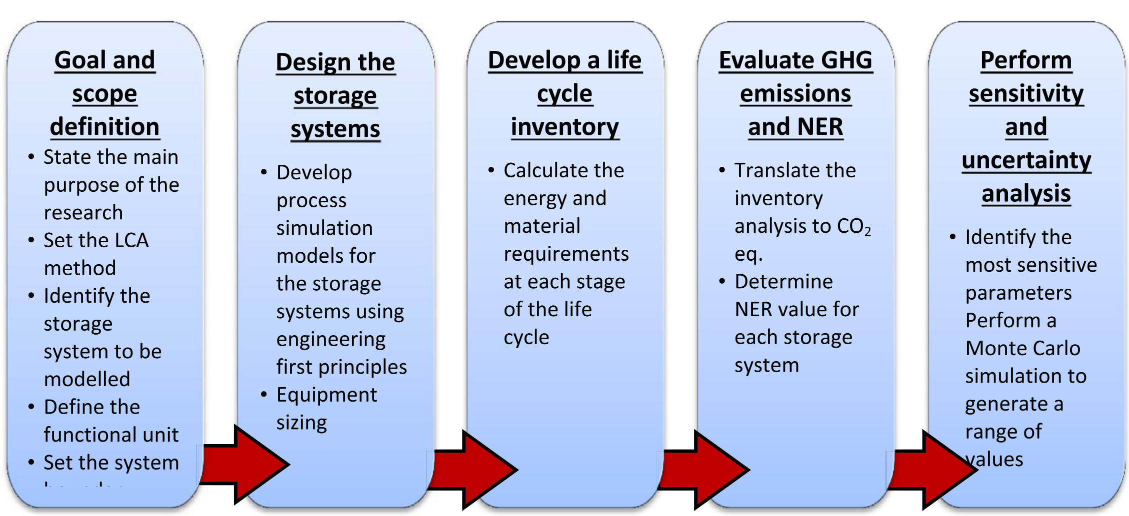

Fig. 1. Greenhouse gas emissions and net energy ratio assessment framework.

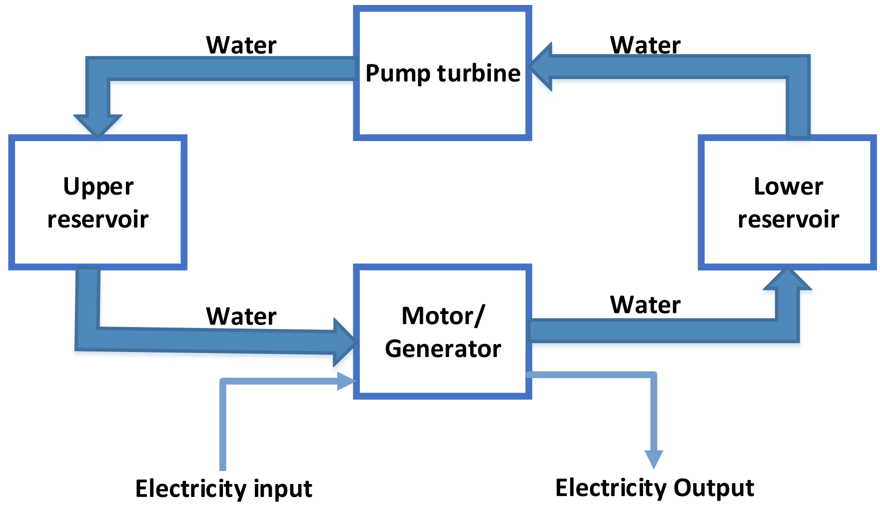

Fig. 2. Pumped hydro storage system diagram.

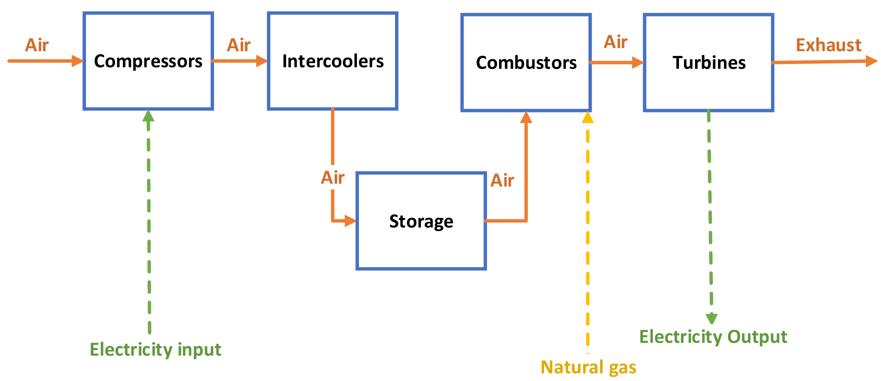

Fig. 3. Conventional compressed air energy storage system diagram.

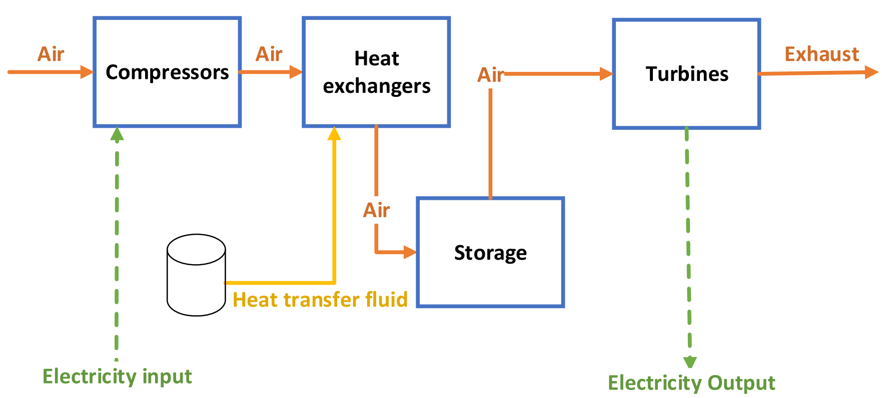

Fig. 4. Adiabatic compressed air energy storage system diagram.

storage consists of two heat exchangers and Dowtherm T as a heat transfer fluid. When there is less demand, the excess electricity is used to compress air that can be heated later with the stored heat in the compressor. The compressed air expands through turbines to generate electricity to meet excess demand.

The system boundary for all three ESSs considered in this study is presented in Fig. 5. Three life cycle phases of storage systems were considered: construction, operation, and decommissioning. The construction phase includes the required equipment and energy to build the storage plant, the site preparation, and the transportation of the equipment to the site. The operational phase comprises the input and output of energy from the storage systems, and the decommissioning phase involves dismantling the equipment and restoring the site to its original condition [21]. The removed equipment disposal/recycling is out of the scope of this study. The functional unit is one kWh of electricity output from the storage system.

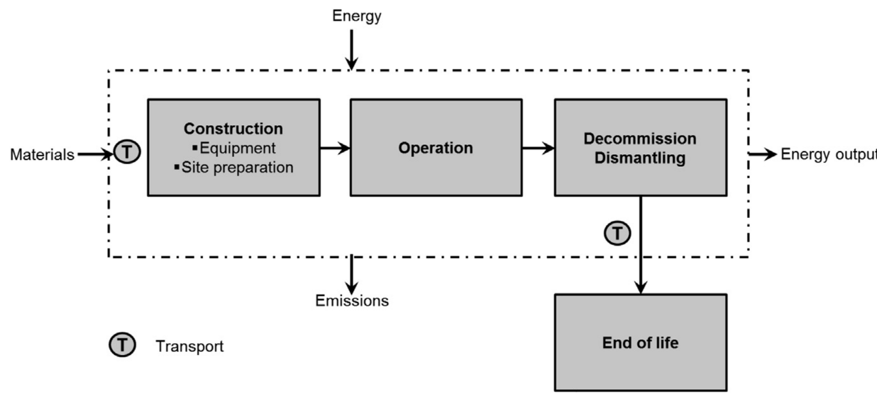

Fig. 5. MESS system boundary.

2.2. Process simulation

The considered technologies were simulated through the development of process models to obtain the base case plant size. (Calculation details are provided in the SI). The MESS defining characteristics were inputs in the simulation model to obtain the individual equipment size. The material and energy required to build equipment of specific sizes were obtained by linearly scaling the data from the literature. The transportation of equipment to the plant site was also considered in the analysis. Then, the total amounts of materials and energy required to build a storage facility of a specific size were calculated to compile materials and energy inventory data.

Base case scenarios were established by simulating PHS and CAES plants [20]. The simulations are described in detail below.

The key parameters for the PHS simulation model are presented in Table 1. The database of existing PHS plants in the US was created by compiling data [22,23]. One of the facilities considered for building database is the Bath County PHS facility, which is the world's largest storage facility with a capacity of 3003 MW and 6 units. The head and volume flow rates, the most important characteristics in defining the power capacity of a PHS facility, are 300 m and 40 m^3/s, respectively [22,23]. Both values are the averages from Refs. [18,19].

The ambient air temperature and pressure for C-CAES are assumed to be 288.15 K and 1 bar, respectively. The key parameters for the simulation are presented in Table 2. The modeled plant consists of three compressors and two turbines. The compressor ratio is 4:1 and the storage cavern is assumed to operate between 45 and 70 bar [24]. The discharge pressure of the first turbine was optimized based on the maximum power output from the plant and was found to be 10 bars.

The A-CAES simulation model was developed using the parameters presented in Table 3. The modeled plant consists of two compressors and two turbines. The compressor ratio was taken to be 13:1 and the storage cavern was assumed to operate between 140 and 160 bar [25]. Higher cavern pressures are required for an A-CAES plant than a C-CAES plant as there is no additional fuel input to heat the compressed air. The discharge pressure of the first turbine was optimized based on maximum power output from the plant and found to be 15 bars.

The simulations results in power capacities of 118 MW, 81 MW, and 60 MW for base case PHS, C-CAES, and A-CAES, respectively. These system sizes are determined by input parameters used in simulations.

2.3. Life cycle inventory assessment

This section provides detailed considerations and inventory results of all the processes and unit operations used in the PHS and CAES base case scenarios to create material and energy inventories.

2.3.1. Pumped hydroelectric storage

The PHS inventory includes two reservoirs (lower and upper), a dam on each reservoir, a penstock, anchors, a pump turbine, a motor and generator, and explosives.

2.3.1.1. Reservoirs. The volume of each reservoir is 518,400 m^3 and is calculated based on the amount of water required for one complete operation cycle of a PHS plant. The height of each reservoir is estimated to be 30 m. It is assumed that the volume of earth material removed to create the reservoir is 10% of the volume of the reservoir. The density of the material removed is considered to be 1440 kg/m^3 [26]. 0.73 g of dynamite is required per kg of rock mined [16]. It is also assumed that material removed is transported 50 km from the site by a truck. The truck energy consumption is assumed to be 3 MJ per ton-km [27].

Table 1
Input parameters for pumped hydro storage simulation.

Stream/Component	Parameter	Value	Units	Reference/remarks
Water	Head	300	m	[7,19]
	Flow rate	40	m^3/s	[19,20]
	Velocity of flow	5	m/s	[19,20]
Pump turbine	Efficiency (pumping mode)	0.91		[21,22]
	Efficiency (generation mode)	0.9205		[21,23]
Other losses	Pipe, frictional, evaporation	0.02		[24]
Motor/generator	Motor efficiency	0.984		[22,23]
	Generator efficiency	0.984		[22,23]
Transformer	Efficiency	0.993		[22,23]
Hours of operation	Pumping mode	12	hours	Assumed

Table 2
Input parameters for conventional compressed air energy storage simulation.

Stream/Component	Parameter	Value	Units	Reference/Remarks
Air	Inlet temperature	288.15	K	Standard conditions
	Pressure	1	bar	Standard conditions
	Flow rate	100	kg/s	Assumed
	Specific heat ratio	1.4		[26]
	Specific gas constant	287	J/kg K	[27]
Natural gas	Inlet temperature	288.15	K	Standard conditions
	Pressure	1	bar	Standard conditions
	Lower heating value	48120	kJ/kg	[28]
Compressor	Compression ratio	4.3		[25]
Intercooler	Effectiveness	0.8		[29]
	U value (air to water)	200	$W/(m^2K)$	[24,30]
Storage cavern	Inlet pressure	70	bar	[31]
	Outlet pressure	45	bar	[31]
	Temperature	303.15	K	Assumed
Recuperator	Effectiveness	0.8		[29]
	U value (air to air)	150	$W/(m^2K)$	[24,30]
Turbine 1	Intel temperature	823.15	K	[32]
	Discharge pressure	10	bar	[32]
Turbine 2	Operating temperature	1098.15	K	[32]
	Turbine discharge pressure	1	bar	[32]
Hours of operation	Compression mode	12	hours	Assumed

Table 3
Input parameters for the adiabatic compressed air energy storage model.

Stream/Component	Parameter	Value	Unit	Comments/Remarks
Air	Inlet temperature	288.15	K	Standard conditions
	Pressure	1	bar	Standard conditions
	Flow rate	100	kg/s	Assumed
	Specific heat ratio	1.4		[26]
Dowtherm T	flow rate (kg/s)	40	kg/s	Assumed
	Initial temperature	288.15	K	Standard conditions
Compressor	Compression ratio	13.1		[33]
Heat exchanger	Effectiveness	0.9		[29]
	U value	200	$W/(m^2K)$	[30,34]
Storage cavern	Inlet pressure	160	bar	[33]
	Outlet pressure	140	bar	[33]
	Temperature	298.15	K	Assumed
Turbine 1	Discharge pressure	15	bar	[33]
Turbine 2	Discharge pressure	1	bar	[33]
Hours of operation	Compression mode	12	hours	Assumed

2.3.1.2. Dams. Dams are built on both the upper and lower reservoirs. The height and width of the upper dam are assumed to be 35 m and 50 m, respectively [22]. The height and width of the lower dam are 25 m and 40 m, respectively [22]. The dam type is concrete gravity [28]. The amount of concrete required for each dam is calculated based on its dimensions.

2.3.1.3. Facility. The amount of concrete required for the facility is calculated based on the amount required for the dams. 0.71 kg of concrete is used in the dam construction per unit kg concrete used for the overall hydro plant [29].

2.3.1.4. Pump-turbine. The calculated capacity of the pump turbine is 118 MW. It is assumed to be composed of 50% carbon steel, 45% stainless steel, and 5% copper [30]. The 465 MW unit pump turbine used in the Bath County facility in the US weighs 87 tons [31]. The pump turbine weight in this study was calculated assuming a linear relation between the weight and capacity of the pump turbine.

2.3.1.5. Motor/generator. The material and energy requirements for the motor and generator were obtained from the ecoinvent database [32]. A linear relation between weight and capacity of the motor and generator was assumed to fulfill the size requirement.

2.3.1.6. Penstock. An on-surface penstock supported by concrete anchors was chosen for the PHS facility [33]. The length and diameter of the penstock, determined through the technical simulation, are 424 m and 3 m^3, respectively. The penstock thickness is calculated using Equation (3) [33]:

$$t = \frac{p^*d}{2^*s} \tag{3}$$

where t is the thickness of the penstock, p is the maximum pressure, d is the diameter of the penstock, and s is the maximum allowable stress. The maximum allowable stress is 20 KSI [33] and the penstock material is assumed to be steel [33].

2.3.1.7. Anchors. The penstock is supported by concrete anchors spaced 90 m apart. Each has a volume of 80 m^3 [28]. The density of the concrete is considered to be 2400 kg/m^3 [34].

2.3.1.8. Vegetation removal impact. PHS plant construction occupies a vast area and requires the removal of existing vegetation or forest. On average, a new forest absorbs 2.5 tons of carbon per acre annually [35]. Thus, PHS construction indirectly results in a release of GHG emissions that would otherwise have been absorbed by the existing forest over the years.

2.3.1.9. Transportation. All the construction material and equipment are transported to the plant site by truck and train. The transportation data for PHS was extracted from the literature [29]. Energy consumption in the form of electricity for the train and diesel for the truck is 0.5 and 3.0 MJ per tonne-kilometre, respectively [27]. Average distances of 300 km by train and 50 km by the truck are assumed. The summary of material and energy requirement for a PHS facility is presented in Table 4.

2.3.2. Compressed air energy storage

The C-CAES and A-CAES inventories are presented in Tables 5 and 6, respectively.

2.3.2.1. Compressor. The C-CAES has three compressors, each with a compression ratio of 4:1. The three compressors have power ratings of 17.25, 17.57, and 17.89 MW. The A-CAES plant has two compressors with a compressor ratio of 13:1 and power ratings of 39.69 MW and 45.36 MW. The materials and energy requirements were calculated using the data from an axial compressor in the ecoinvent database, assuming a linear relationship [32].

2.3.2.2. Turbine. The power capacities of the two turbines are 28 MW and 53 MW for C-CAES and 27 MW and 33 MW for A-CAES. The turbines are linearly scaled from available data for a gas turbine in the ecoinvent database [32].

2.3.2.3. Cavern. This analysis assumes an underground salt cavern for both C-CAES and A-CAES. The cavern is formed by drilling holes into the ground to the required depth using a drill rig. Then water, extracted by pumps to reach the required volume, is supplied to the cavern to form a brine solution [36]. Carbon steel and stainless steel pipes with 16–48 inches in diameter are installed in the drilled holes [37]. The space between the pipes is filled with concrete to consolidate the foundation [37].

2.3.2.4. Heat exchangers. The amount of materials and energy required for heat exchangers was calculated from published data [37]. The operating temperatures of the heat exchangers are below 200 °C in C-CAES and above 200 °C in A-CAES. The materials required for C-AES heat exchangers are carbon steel for the pipes and outer structure and aluminum for the fins [38]. Because of the high operating temperature, the recuperator is made of stainless steel. A-AES heat exchangers are made entirely of stainless steel [38].

Table 4
Developed PHS life cycle inventory list.

Equipment	Material	Amount	Units
Dams	Concrete	77625000	kg
Pump-turbine	Carbon steel	457688	kg
	Stainless steel	411919	kg
	Cooper	45769	kg
Explosives	Dynamite	753	kg
Penstock	Steel	1016425	kg
Anchors	Concrete	906240	kg
Motor/Generator	Cast iron	350217	kg
	Copper	150093	kg
Reservoirs	Diesel	2940504	L
	Energy	111974400	MJ
Vegetation removal Impact	Area	103680	m^2
	Impact	61.8	per m^2 annum
Transportation	Electricity	4491951	MJ
	Diesel	466637	L
Facility construction	Electricity	33829011	MJ
	Diesel	1942692	L
	Concrete	31705986	kg

Table 5
Developed C-CAES life cycle inventory list.

Equipment	Material	Amount	Units
Turbines	Concrete	969185	kg
	Copper	40383	kg
	Steel	383636	kg
	Stainless steel	20191	Kg
	Electricity	378790	MJ
	Diesel	313910	L
Compressors	Aluminum	77306	kg
	Cast Iron	298680	kg
	Copper	105417	kg
	Steel	737916	kg
	Stainless steel	87847	kg
	Rubber	1581	kg
Motor/Generator	Cast Iron	240277	kg
	Copper	102976	kg
	Electricity	74708	MJ
	Diesel	91476	L
Cavern	Carbon steel	266464	kg
	Stainless steel	45030	kg
	Concrete	578964	kg
	Electricity	2846251	MJ
Natural gas infrastructure	Stainless steel	79463	kg
	Diesel	3508772	L
Heat exchangers	Carbon steel	223827	kg
	Aluminum	8481	kg
Transportation	Electricity	196011	MJ
	Diesel	18530	L

Table 6
Developed A-CAES life cycle inventory list.

Equipment	Material	Amount	Units
Turbines	Concrete	719494	kg
	Copper	29979	kg
	Steel	284800	kg
	Stainless steel	14989	kg
	Electricity	281202	MJ
	Diesel	233037	L
Compressors	Aluminum	124747	kg
	Cast Iron	481979	kg
	Copper	170110	kg
	Steel	1190770	kg
	Stainless steel	141758	kg
	Rubber	2552	kg
Motor/Generator	Cast iron	253039	kg
	Copper	108445	kg
	Electricity	78676	MJ
	Diesel	96335	L
Cavern	Carbon steel	266464	kg
	Stainless steel	45030	kg
	Concrete	578964	kg
	Electricity	4592975	MJ
Dowtherm T storage tank	Stainless steel	375118	kg
Heat exchangers	Carbon steel	213664	kg
	Aluminum	11308	kg
Transportation	Electricity	230255	MJ
	Diesel	21768	L

2.3.2.5. Motor/generator. The motor/generator capacities for C-CAES and A-CAES plants are 81 MW and 60 MW, respectively. The material and energy data were extracted from the ecoinvent database [32].

2.3.2.6. Natural gas infrastructure. The natural gas infrastructure includes pipeline for the transportation of natural gas to the plant site and storage tanks to store the natural gas at the site and supply to the turbines. The storage tanks are made of stainless steel and store natural gas for daily operations. The pipeline is assumed to be 1000 km long. A site where there is an abundance of wind could be an ideal site to integrate a MESS with a wind facility [39]. The dimensions of the pipeline are based on a target velocity of 1.4 m/s [40].

2.3.2.7. Dowtherm T storage tanks. Two stainless steel storage tanks were assumed to store Dowtherm T fluid. The dimensions of the tanks are based on the amount of Dowtherm T fluid required.

2.3.2.8. Transportation. All the construction materials and equipment are transported to the plant site in the same manner as for the PHS plant.

The summary of material and energy requirements for C-CAES and A-CAES is presented in Tables 5 and 6, respectively.

The NER is defined as the ratio of total energy output to total energy input to the system over the life of the storage plants and is calculated with Equation (4). The input energy includes construction, operation, and maintenance energy.

$$NER = \frac{Output\,energy}{Contruction\,energy + Maintenance\,energy + Operational\,energy} \tag{4}$$

2.4. Sensitivity and uncertainty analyses

Sensitivity analysis was conducted using the Morris and Sabol methods to investigate the effects of input process parameters on the NERs and GHG emissions from the considered storage facilities. The selected parameters for PHS are the head, flow rate, pump efficiency, turbine efficiency, material emissions, plant life, and daily hours of operation. For C-CAES and A-CAES, the following were selected: air inlet temperature, flow rate, compressor efficiency, turbine inlet temperature, material emissions, plant life, daily hours of operation, and natural gas emission factor.

Uncertainty analysis was performed to evaluate the effect of a simultaneous change in multiple input parameters on the NERs and the life cycle GHG emissions. A Monte Carlo simulation was conducted through ModelRisk software [41] to evaluate the range of emissions associated with storage facilities. All the uncertain process input variables were identified with their highest and lowest ranges. The range of input variables is presented in Table 7. A random sample was selected from the range of input variables to obtain final outputs and the process was iterated 100,000 times to obtain the final output distribution.

3. Results and discussion

The results and discussion section is organized as follows. First, the NER results are presented and discussed. Second, the GHG emission results that show the life cycle stage contribution and detailed analysis of the influence of electricity sources on the overall results are described. The last section is dedicated to sensitivity and uncertainty analysis results.

3.1. Net energy ratio results

A Sankey diagram of one operation cycle of PHS, C-CAES, and A-CAES is shown in Fig. 6. The diagram includes the total energy inputs and outputs and the losses associated with the transmission of electricity from generation site to storage site and then to the end user. A 5% transmission loss was also considered in the energy flow [7].

Electricity and natural gas are the main sources of energy. The energy consumed and produced over the life cycle was obtained based on plant life and daily hours of operation. The lifetimes of PHS and CAES plants were taken as 60 and 40 years, respectively [42,43]. It is assumed that the storage facility is operated 12 h a day, 300 days a year. The net energy inputs required by PHS, C-CAES, and A-CAES to deliver energy outputs of 60, 81, 118 MW were estimated to be 1413, 1782, and 1021 kWh, respectively. The corresponding NERs are 0.778, 0.542, and 0.702, respectively. When a 5% transmission loss is considered, the NERs are 0.74, 0.52, and 0.67, respectively. It is important to mention that transmission loss affects the delivered energy during the transport of electricity, and this value varies depending on the distance of electric projects. The NERs of PHS and A-CAES are considerably higher because losses are minimal compared to C-CAES. The energy losses in the pump and turbine together make up 16% of the total input energy for PHS. While most of the losses in PHS are due to the resistance from the electrical devices and friction losses, installing high efficiency electrical devices, motors, and adjustable speed drives are options to reduce losses. In C-CAES, the intercooler losses account for a significant part of the total input energy (29%), mainly due to the dissipation of the compression heat. This indicates that a huge percentage of the electrical energy supplied to the compressor is lost to the environment in the form of waste heat. A significant reduction in energy losses can be achieved by lowering the compression ratios at each stage and adding more compression stages. However, the additional compressor needed to trade off heat losses and compression ratios will lead to an increase in capital cost and emissions associated with material production. Unlike in C-CAES, heat exchanger losses are highest in A-CAES, accounting for 29.8% of input energy. The energy losses in the heat exchangers are irreversible. They are mainly due to entropy generation in the system that result from the variations in the operating conditions of the streams exchanging heat. The exhaust gases from the C-CAES and A-CAES turbines also contribute considerable losses. In case of A-CAES, where a heat recovery system is available, a heat recovery device can be installed to recover heat for storage. The identified areas of losses are keys to improving NER and reducing GHG emissions in each of the energy storage systems.

3.2. GHG emissions contributions

The comparative LCA results for the three storage systems are presented in Fig. 7. With its relatively low GHG emissions footprint, PHS offers a higher environmental benefit. C-CAES appears to have the lowest environmental performance, 75% higher GHG emissions than PHS per kWh. The largest contribution in the case of C-CAES is due to the consumption of natural gas. Unlike A-CAES, where the heat due to compression work is used to preheat the compressed air, C-CAES uses natural gas to meet the gas turbine specification in order to generate electricity.

Fig. 7 (A) and (B), respectively, show the global GHG emission contributions by life cycle stages and energy and material requirements. From the three main life cycle stages considered, the GHG emissions are highly dominated by the operational stage in all the energy storage systems. The construction and decommissioning stages have marginal impact on global GHG emissions in all cases. There is a general agreement among LCA practitioners that inputs that contribute less than 5% of the total impacts are assumed to have no effect and so can be excluded from the system. However, it is important to note that excluded inputs may make a significant contribution in environmental areas other than GHG emissions such as human health, acidification, and resource depletion, so additional cut-off criteria need to be applied. In this particular study, the operational phase appears to be the hotspot that needs further investigation to better interpret the results and understand

Table 7
Uncertainty analysis input parameters.

System	Parameters	Min value	Base value	Max value	Units	Reference
PHS	Head	100	300	600	m	[19,20]
	Efficiency (pump)	0.9	0.91	0.92		[21,22]
	Efficiency (turbine)	0.916	0.9205	0.925		[21,23]
	Hours of operation (pumping)	10	12	13	hours	
	Flow rate (m^3/s)	20	40	80	m^3/s	[19,20]
	Velocity of flow	4	5	10	m/s	[19,20]
	Plant life	50	60	70	years	[5]
	Motor efficiency	0.978	0.984	0.99		[22,23]
	Generator efficiency	0.978	0.984	0.99		[22,23]
	Transformer efficiency	0.99	0.993	0.996		[22,23]
C-CAES	Flow rate	95	100	105	m^3/s	
	Air inlet temperature	273.15	288.15	298.15	K	
	Turbine 1 temperature	810.15	823.15	823.15	K	[31,32]
	Turbine 2 temperature	1073.15	1098.15	1144.15	K	[31,32]
	Plant life	35.00	40.00	50.00	years	[5]
	Hours of operation	10.000	12.00	13.00	hours	
A-CAES	Flow rate	95	100	105	m^3/s	
	Air inlet temperature	273.15	288.15	298.15	K	
	Plant life	35	40	50	years	[5]
	Hours of operation	10	12	13	hours	

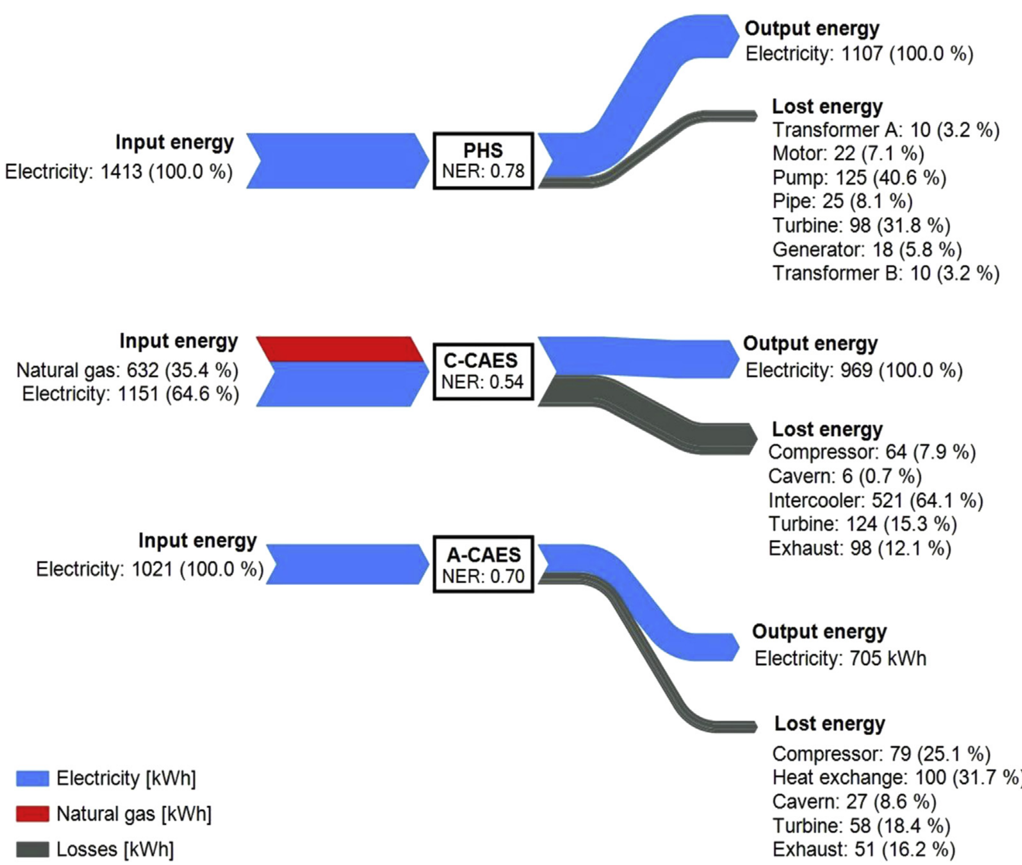

Fig. 6. Energy flow diagram for single PHS, A-CAES and C-CAES cycle.

their implications for decision-making.

Energy consumption in the form of electricity is the key driver, while the contributions from materials are minimal. Since electricity is the input that most influences the overall results, the implications of different electricity sources were investigated. Fig. 8 shows the effects of a change in the electricity mix on the total GHG emission results. Compared with Canada's average electricity mix, which is considered as a base case, the GHG emission footprints of the storage systems vary significantly depending on the cleanness of the electricity sources. The change is more considerable in PHS and A-CAES, where the operational phase emissions are highly dominated by electricity use, more than 96% fewer GHG emissions when the Quebec electricity mix considered. C-CAES also exhibited changes in GHG emissions, though not high like PHS and A-CAES. Natural gas also has a key contribution in terms of GHG emissions of the C-CAES system.

Fig. 8 also highlights the fact that comparative assessment results could differ depending on the source of electricity. The high

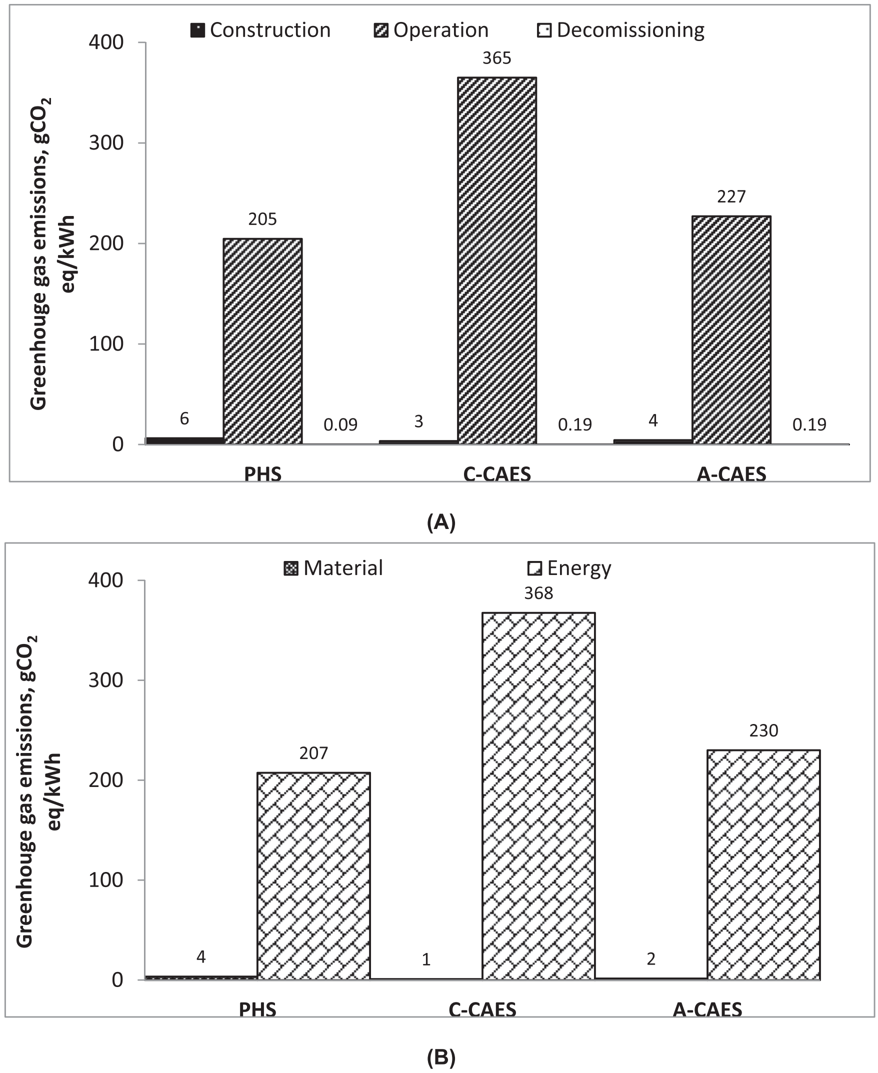

Fig. 7. Life cycle greenhouse gas emissions of PHS, A-CAES and C-CAES.

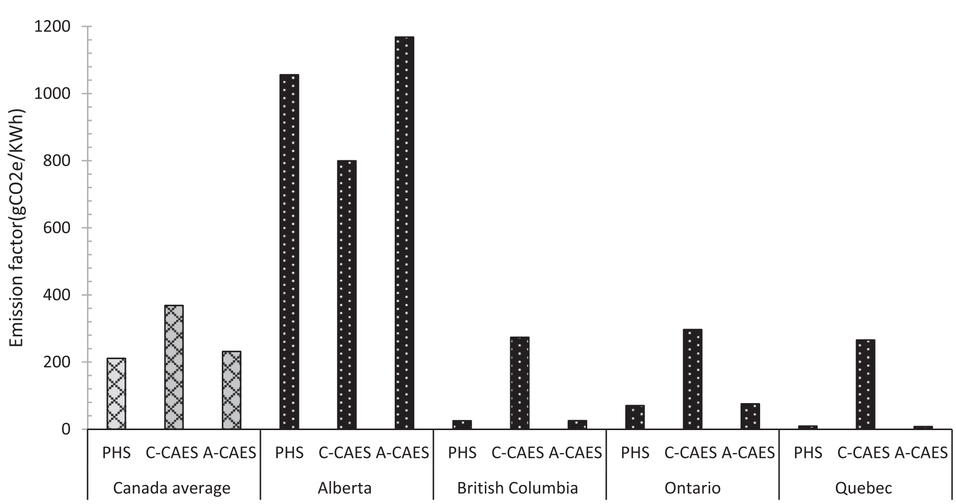

Fig. 8. Total GHG emissions by electricity source.

GHG emissions per kWh of electricity generation in Alberta make C-CAES a better choice than PHS and A-CAES. The energy mix of C-CAES is another factor to consider. C-CAES uses natural gas and electrical energy at a ratio of 1:1.8. Since the emission factor of natural gas does not change significantly irrespective of location, a large increase in the electricity emission factor would thus favor C-

CAES over PHS and A-CAES.

Some of the findings in this study were compared with those of Denholm and Kulcinshi [7] and Oliviera et al. [12]. Denholm and Kulcinshi reported the life cycle GHG emissions from PHS and C-CAES to be 5.6 and 292 gCO_2e/kWh, respectively. The results reported for C-CAES are in the range of values reported in this study, while the PHS results vary widely. The difference in PHS emissions may be due the different sources of electricity used, emissions factor, and inaccuracy resulting from the use of aggregated data. On the other hand, Oliviera et al. reported the construction emissions for PHS as 5 gCOe/kWh and 7 gCO_2e/kWh for C-CAES. The respective life cycle GHG emissions for PHS and C-CAES are ~5–650 gCO_2e/kWh and ~10–750 gCO_2e/kWh; these results largely depend on the source of electricity [12]. These results are in good agreement with this study's.

One of the key applications of LCA is to support decisions on the superiority of one product over its alternative products that provide comparative functionality based on their environmental performance. While performing comparative LCA, care must be taken in the interpretation of the results. As suggested by ISO [44,45], products being compared should have the same system boundary, functional unit, and similar methodological considerations such as allocation rules and input and output data quality. Inconsistent use of electricity and different sources for different storage systems could result in misleading conclusions. Results from comparative assessment need to show the sensitivity and sources of uncertainty for better interpretation.

3.3. Sensitivity and uncertainty analyses results

The interactions of input parameters and their impacts on the GHG emissions and NERs of the energy storage systems were examined. The Morris method was applied to identify the non-influential parameters on the GHG emissions and NERs of the energy storage systems. The sensitivity analysis results of the GHG emissions and NER for each storage system follow similar trends. PHS, C-CAES, and A-CAES are most sensitive to pump turbine efficiency, combustion temperature, and air flow rate, respectively, due to their relatively high standard deviation and mean values in the Morris analysis. The high absolute mean and standard deviation values of these parameters indicate that they are the key input parameters influencing change in NERs and GHG emissions associated with the energy storage systems. Some other input parameters such as head and water volume flow for PHS, plant life and hours of operations for C-CAES, and air flow rate, and plant life and operation hours for A-CAES have relatively high standard deviation but low mean values, indicating that there can be large interactions or non-linear effects with other input parameters based on their position in the Morris plot. On the other hand, other input parameters with comparatively lower absolute mean and standard deviation values are identified as non-influential inputs parameters and are thus eliminated from uncertainty analysis. The NER and GHG emission uncertainty analysis results for PHS, C-CAES, and A-CAES are shown in Figs. 9 and 10, respectively. The results show probability ranges in uncertainty in NERs from 0.769 to 0.786, 0.534–0.541, and 0.699–0.720 for PHS, C-CAES, and A-CAES, respectively. It is clear that PHS has the highest NER followed by A-CAES and C-CAES. A Sobol sensitivity analysis was conducted to show the input parameters with the largest impact on the output uncertainty for each energy storage system. The input parameters influencing the uncertainty in the NERs of PHS, C-CAES, and A-CAES are turbine efficiency, combustion temperature, and air flow rate, respectively. The contributions from the pump turbine efficiency, combustion temperature, and air flow rate to their respective storage systems are 40.6%, 72.6%, and 99.4% of the overall range of uncertainty in the NERs, respectively. On the other hand, the probability ranges in emissions' uncertainty are from 269.75 to 276.04 gCO2e/kWh, 397.23–403.10 gCO2e/kWh, and 296.12–308.85 gCO2e/kWh for PHS, C-CAES, and A-CAES, respectively. GHG emissions are highest in C-CAES and lowest in PHS. The input parameter influencing the uncertainty in emissions of PHS is the head, while C-CAES and A-CAES are sensitive to operation hours. Considering the present uncertainty analysis results, the performance of PHS is much better than C-CAES and A-CAES. However, it is important to mention that the results could be different depending on the sources of electricity used.

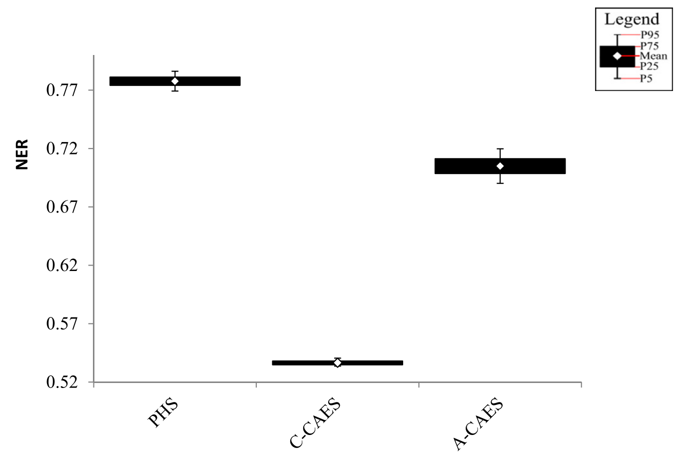

Fig. 9. Net energy ratio uncertainty analysis.

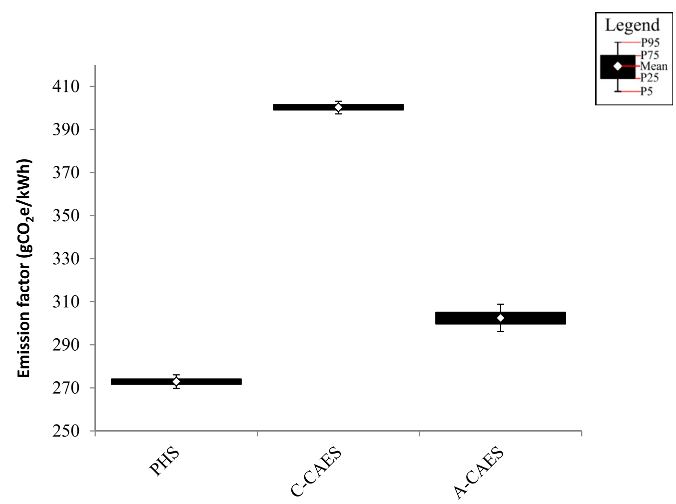

Fig. 10. GHG emissions uncertainty analysis.

4. Conclusion

The objective of this study was to develop NERs and evaluate the life cycle GHG emissions of PHS, C-CAES, and A-CAES. To that end, the contribution of each life cycle stage and the energy and material requirements for each storage technology were investigated, and life cycle inventories were established. Simulation models were developed to model PHS and CAES systems and determine the required equipment sizes.

From the three main life cycle stages considered, the GHG emissions are highly dominated by the operational phase in all the energy storage systems. Construction and decommissioning stages have minimal importance to the global GHG emissions in all cases. Again, it was observed that energy consumption in the form of electricity is the key driver, while the contributions from materials are minimal. PHS has the highest energy output of the three technologies for the same amount of energy storage based on NER. Further improvement in turbine technology will increase the NER for PHS, C-CAES and A-CAES. C-CAES has the highest GHG emissions footprint among the three technologies. The high emission factor for C-CAES is due to its hybrid nature (i.e., natural gas needs to be combusted during the operation stage). The sensitivity analysis results of the GHG emissions and NER for each storage system follow similar trends. The PHS, C-CAES, and A-CAES results are most sensitive to pump turbine efficiency, combustion temperature, and air flow rate, respectively. To consolidate the developed model and mitigate risk, an uncertainty analysis was performed, which showed that PHS performs better than C-CAES and A-CAES. Finally, it can be said that the environmental performance of a MESS can be influenced by the grid electricity mix.

The results of this LCA provide useful insight on the NERs and life cycle GHG emissions of PHS and CAES. The detailed quantitative emissions and energy analysis provided in the study will be helpful in decision making regarding investment and formulating regulations for large MESSes.

The goals of this work are to apply the developed method to other energy storage technologies, to perform a process optimization on the storage systems to investigate the potential for further improvement, and to identify suitable sites for building pumped hydro storage and compressed air energy storage facilities in Canada and globally.

Acknowledgement

The authors thank the NSERC Energy Storage Technology (NEST) Network (RYERU NSERC 468468 Kumar) and the University of Alberta (UOFAB VPRGRF NEST KUMAR) for the financial support provided to carry out this research. We are also grateful to the NSERC/Cenovus/Alberta Innovates Associate Industrial Research Chair in Energy and Environmental Systems Engineering and the Cenovus Energy Endowed Chair in Environmental Engineering for providing financial support for this project. The authors thank Astrid Blodgett for editing this paper.

Appendix A. Supplementary data

Supplementary data to this article can be found online at https://doi.org/10.1016/j.energy.2018.12.183.

References

[1] Climate change 2014: mitigation of climate change in climate change. 2014. p. 1246.
[2] National inventory report 1990-2014: greenhouse gas sources and sinks in Canada. 2016 [Canada].
[3] World energy resources. 2016 [England and Wales].
[4] Gielen D. Energy technology perspectives. Paris: International Energy Agency; 2017.
[5] Decourt B, Debarre R. Electricity storage, in leading the energy transition. 2013. p. 98.
[6] How Energy Storage Works. [cited 8 Aug 2017]; Available from: http://www.ucsusa.org/clean-energy/how-energy-storage-works#.WZ3-U1FGmUk.
[7] Denholm P, Kulcinski GL. Life cycle energy requirements and greenhouse gas emissions from large scale energy storage systems. Energy Convers Manag 2004;45(13–14):2153–72.
[8] Hiremath M, Derendorf K, Vogt T. Comparative life cycle assessment of battery storage systems for stationary applications. Environ Sci Technol 2015;49(8):4825–33.
[9] Rydh CJ. Environmental assessment of vanadium redox and lead-acid batteries for stationary energy storage. J Power Sources 1999;80(1):21–9.
[10] Jing Y-Y, et al. Life cycle assessment of a solar combined cooling heating and power system in different operation strategies. Appl Energy 2012;92:843–53.
[11] Oró E, et al. Comparative life cycle assessment of thermal energy storage systems for solar power plants. Renew Energy 2012;44:166–73.
[12] Oliveira L, et al. Environmental performance of electricity storage systems for grid applications, a life cycle approach. Energy Convers Manag 2015;101:326–35.
[13] Sternberg A, Bardow A. Power-to-What?–Environmental assessment of energy storage systems. Energy Environ Sci 2015;8(2):389–400.
[14] Ma T, Yang H, Lu L. Feasibility study and economic analysis of pumped hydro storage and battery storage for a renewable energy powered island. Energy Convers Manag 2014;79:387–97.
[15] Kadiyala A, Kommalapati R, Huque Z. Evaluation of the life cycle greenhouse gas emissions from hydroelectricity generation systems. Sustainability 2016;8(6):539.
[16] Bouman EA, Øberg MM, Hertwich EG. Environmental impacts of balancing offshore wind power with compressed air energy storage (CAES). Energy 2016;95:91–8.
[17] Welsch B, et al. Environmental and economic assessment of borehole thermal energy storage in district heating systems 2018;216:73–90.
[18] Tschiggerl K, Sledz C, Topic MJE. Considering environmental impacts of energy storage technologies: a life cycle assessment of power-to-gas business models 2018;160:1091–100.
[19] Guney MS, Tepe YJR, Reviews SE. Classification and assessment of energy storage systems 2017;75:1187–97.
[20] Kapila S, Oni AO, Kumar A. The development of techno-economic models for large-scale energy storage systems. Energy 2017;140(Part 1):656–72.
[21] CENTER E. Life-cycle energy costs and greenhouse gas emissions for gas turbine power. 2000.
[22] Engineers A.S.o.C. Compendium of pumped storage plants in the United States. New York, NY: American Society of Civil Engineers; 1993. p. 744.
[23] Carson J, et al. Operation and maintenance experiences of pumped-storage plants. Palo Alto, CA (USA): Morrison-Knudsen Engineers, Inc., San Francisco, CA (USA); Electric Power Research Inst.; 1991.
[24] Bozzolani E. Techno-economic analysis of compressed air energy storage systems. 2010.
[25] Jubeh NM, Najjar YS. Green solution for power generation by adoption of adiabatic CAES system. Appl Therm Eng 2012;44:85–9.
[26] Density of some common building materials. 2017 [cited 2017 5 Sep]; Available from: http://www.rfcafe.com/references/general/density-building-materials.htm.
[27] Adams M, et al. European Union emission inventory report 1990–2010 under the UNECE convention on long-range transboundary air pollution (LRTAP). 2012 [EEA technical report].
[28] Norge A. In: Slapgård J, editor. Cost base for hydropower plants; 2012 [Norway].
[29] Flury K, Frischknecht R. Life cycle inventories of hydroelectric power generation. ESU-Services, Fair Consulting in Sustainability, commissioned by€ Oko-Institute eV; 2012. p. 1–51.
[30] The choice of materials for turbines. [cited 2017 July 17]; Available from: http://www.ivt.ntnu.no/ept/fag/tep4200/innhold/The%20choice%20of%20materials.pdf.
[31] Bath County, USA. [cited 2017 July 16]; Available from: http://voith.com/en/markets-industries/industries/hydro-power/pumped-storage-plants/bathcounty_main-11333-11333.html.
[32] Ecoinvent 3.3. 2017 [cited 2017 12 June]; Available from: http://www.ecoinvent.org/.
[33] Iron A, S. Institute, S.P.F. Association. Buried steel penstocks. American Iron and Steel Institute; 1992.
[34] Concrete - properties. 2017 [cited 2017 July 17]; Available from: http://www.engineeringtoolbox.com/concrete-properties-d_1223.html.
[35] Trees improve our air quality. 2017 [cited 2017 July 19]; Available from: http://urbanforestrynetwork.org/benefits/air%20quality.htm.
[36] Succar SW, Robert H. Compressed air energy storage: theory, resources and applications for wind power. 2008.
[37] Pollak R. History of first US compressed-air energy storage (CAES) plant (110 MW 26h) volume 2: construction. Electric Power Research Institute (EPRI); 1994.
[38] Waheed MA, Oni AO. Performance improvement of a crude oil distillation unit. Appl Therm Eng 2015;75:315–24.
[39] Wind energy in Canada. [cited 2017 28 Aug]; Available from:http://www.nrcan.gc.ca/sites/www.nrcan.gc.ca/files/canmetenergy/pdf/fichier/81770/windtrm_resource_map.pdf.
[40] Nimana B, et al. Life cycle analysis of bitumen transportation to refineries by rail and pipeline. Environ Sci Technol 2017;51(1):680–91.
[41] ModelRisk. [cited 2017 10 Nov]; Available from: https://www.vosesoftware.com/products/modelrisk/.
[42] Kousksou T, et al. Energy storage: applications and challenges. Sol Energy Mater Sol Cell 2014;120(Part A):59–80.
[43] Akhil AA, et al. DOE/EPRI 2013 electricity storage handbook in collaboration with NRECA. Albuquerque, NM: Sandia National Laboratories; 2013.
[44] ISO, ISO 14040. International standard - environmental management – life cycle assessment – principles and framework. Geneva, Switzerland: International Organisation for Standardization; 2006.
[45] ISO, ISO 14044. International standard - environmental management – life cycle assessment – requirements and guidelines. Geneva, Switzerland: International Organisation for Standardization; 2006.